Materials Today Communications 33 (2022) 104479

Contents lists available at ScienceDirect

Materials Today Communications

journal homepage: www.elsevier.com/locate/mtcomm

Intrinsic low-dielectric constant and low-dielectric loss aliphatic-aromatic copolyimides: The effect of chemical structure

Jiwon Lee [a,b,1], Sungmi Yoo [a,1], Dongkyu Kim [a], Yun Ho Kim [a,c], Sungmin Park [a], No Kyun Park [a], Yujin So [a,d], Jinsoo Kim [a], Jongmin Park [a,*], Min Jae Ko [b,*], Jong Chan Won [a,c,**]

[a] Advanced Functional Polymers Center, Korea Research Institute of Chemical Technology (KRICT), Daejeon 34114, South Korea
[b] Department of Chemical Engineering, Hanyang University, Seoul 04763, South Korea
[c] KRICT School, University of Science and Technology (UST), Daejeon 34113, South Korea
[d] Department of Chemical and Biomolecular Engineering, Korea Advanced Institute of Science and Technology (KAIST), Deajeon 34141, SOuth Korea

ARTICLE INFO

Keywords:
Low dielectric material
Low dielectric polyimide
Copolyimide
Chain relaxation

ABSTRACT

Low-dielectric polymer materials are becoming essential for 5 G mobile communication to achieve mass transport information without signal loss. Herein, we present an aliphatic–aromatic copolyimide using Priamine 1075 (aliphatic) and m-tolidine (aromatic) as diamines. The branched bulky aliphatic units enlarge the free volume, effectively reducing the dipole moment density, while the aromatic diamine was introduced to prevent polymer chain relaxation under the operating conditions. We observed that there is an optimal composition that regulates the chain movement and density of dipole moments through the control of the polymer chain rigidity and nanostructure. Thus, by tuning the composition, we succeeded in achieving a low-dielectric copolyimide with a dielectric constant (D_k) of 2.63 and dielectric loss (D_f) of 0.0017 at 28 GHz. Combining molecular design and composition control, this study suggests a design factor for advanced copolymers for telecommunication applications with fast signal transport speed and minimum signal loss.

1. Introduction

With the development of internet-based technology, the simultaneous transport of a large amount of information with high accuracy is essential in 5 G communication networks [1]. For new-generation communication platforms, the combination of high-frequency signals (>6 GHz) and low-dielectric materials is necessary to achieve fast-speed transportation. The severe signal loss caused by absorbing and reflecting high-frequency electromagnetic waves in the insulation substrate also needs to be minimized [2]. Therefore, an interlayer dielectric material with a low dielectric constant (D_k <3.0) and dielectric loss (D_f <0.005) is essential. In addition, mechanical and thermal stability should be achieved to ensure the reliability of device operation. Polymer-based dielectric materials have been suggested as attractive candidates because of their excellent mechanical properties, ease of processing, and relatively low dielectric constant compared to those of inorganic materials [2–6]. Low-dielectric polymers, such as fluorinated and aliphatic polymers, have been suggested as the material for substrate, and insulation layer. However, their insufficient thermal and mechanical stability and unsatisfactory dielectric properties remain challenges that need to be overcome.

To satisfy the required properties of polymer materials, we selected polyimide (PI) as the synthetic platform. The imide functional group consists of two acyl groups (-C═O-) bound to nitrogen (-N-) that strongly interact via non-covalent interactions to provide strong mechanical and thermal stability [7,8]. This stability is maximized by using aromatic units that enhance the chain rigidity and non-covalent interactions (e.g., π–π stacking), resulting in excellent thermal stability (≤500 °C), mechanical properties (Young's modulus, E ≥ 100 MPa), and chemical resistance. Therefore, PIs have been widely used for electronic packaging and as electrical insulation materials in the microelectronics industry [3,9,10]. However, the electron-rich chemical structure and closely stacked nanostructure of these materials usually result in unsatisfactory dielectric properties, with a high D_k, in the range of 3.0–3.6, that is difficult to apply in 5 G applications [11,12].

The introduction of bulky aliphatic units has been suggested to

* Corresponding authors.
** Corresponding author at: Advanced Functional Polymers Center, Korea Research Institute of Chemical Technology (KRICT), Daejeon 34114, South Korea.
E-mail addresses: jmp1208@krict.re.kr (J. Park), mjko@hanyang.ac.kr (M.J. Ko), jcwon@krict.re.kr (J.C. Won).
[1] Equally contributed

https://doi.org/10.1016/j.mtcomm.2022.104479
Received 9 May 2022; Received in revised form 23 August 2022; Accepted 14 September 2022
Available online 15 September 2022

improve the dielectric properties of PIs. The unsaturated aliphatic unit is known to display low dipole strength [13], while the bulky architecture sterically hinders interchain packing by generating free volumes [14]. Thus, the dipole density effectively decreases, resulting in a significant reduction in D_k and D_f at a relatively low frequency (~1 GHz) [15,16]. However, when the signal transporting frequency reaches 10–10^3 GHz, the two values fall within the range of the kinetic motion—such as bending, stretching, and rotational movements—of the aliphatic units [17–19]. These undesirable energy dissipations cause energy loss via thermal and motional energy, resulting in severe signal losses by the insulation substrate. Therefore, to achieve PIs with low D_k and D_f values, the chemical structure should be designed to contain a highly branched aliphatic unit and arrest the random motion of the components, simultaneously.

In this study, we designed a copolyimide containing the dimer diamine (Priamine 1075) and m-tolidine (mTB) as aliphatic and aromatic dianhydrides, respectively. The dimer diamine is a branched and bulky aliphatic diamine with a large free volume, which was expected to decrease the dielectric constant toward a D_k value of 2.5 [20,21]. Moreover, we incorporated mTB to impede chain movement by enhancing interchain interaction. 4,4′-bisphenol A dianhydride (BPADA) which enlarges a free volume by hindering interchain packing was chosen as a dianhydride monomer to minimize dielectric values of the resulting polymer. Subsequently, by copolymerizing BPADA, Priamine 1075 and mTB, a series of copolyimides were synthesized with varying the ratio of the aromatic and aliphatic building units. All copolyimides were soluble in common organic solvents, which allowed them to be shaped by the solution-casting process. The synthesized copolyimides showed a linear change in D_k, from 2.5 to 2.8, at 10, 28, and 40 GHz, proportional to the ratio between the aliphatic and aromatic building units. Notably, a minimum D_f of 0.0017 was observed at 28 GHz for the 30 mol% mTB units, suggesting the presence of an optimal composition for the novel dielectric property. Differential scanning calorimetry (DSC), dynamic modulus analysis (DMA), and wide-angle X-ray scattering (WAXS) were employed to elucidate the thermal transitions and nanostructures of the copolyimides. Using the afforded data, we developed a correlation between the dielectric properties and nanostructure of the polymer materials and addressed the importance of molecular-level design to achieve the desired physical properties. Our rational chemical structure design for copolyimide will contribute to achieving the novel dielectric properties of substrate materials for microelectronic devices in next-generation telecommunication applications including a flexible copper clad laminate (FCCL) antenna.

2. Experimental Section

2.1. Materials

Unless otherwise stated, the chemicals were used as received without further purification. 4,4-(4,4-Isopropylidenediphenoxy)diphthalic anhydride (BPADA, ≥99.0%) and m-tolidine (mTB, ≥99.0%) were purchased from Changzhou Sunchem Pharmaceutical Chemical Material Co., Ltd. (Changzhou, China). The dimer diamine (Priamine 1075, ≤100%) was purchased from Croda (Plainsboro, NJ, US). Cyclohexanone (99%) and toluene (99.5%) were purchased from Duksan (Ansan, Korea) and used without purification.

2.2. Methods

The ^{1}H nuclear magnetic resonance (^{1}H NMR) spectra were recorded on a Bruker Advance 400 MHz spectrometer (Bilerica, MA, US) using a residual solvent signal as the internal standard. Fourier transform infrared (FT-IR) spectra were obtained using a Bruker Alpha-P spectrophotometer in the range of 650–4000 cm^{-1} under ambient conditions. Size exclusion chromatography (SEC) was conducted in a tetrahydrofuran (THF) solution at 40 °C, with a flow rate of 0.6 mL min^{-1}, using a Waters e2695 high-performance liquid chromatograph (Milford, MA, US) equipped with four Waters Styragel high-resolution (HR 0.5, 1, 4E, 4) columns (7.8 ×300 mm) with a molar mass in the range of 100–10,000,000 g mol^{-1}. The number- and weight averaged molar masses (M_n and M_w) and dispersity ($Đ$) of the polymers were calculated relative to linear polystyrene (PS) standards from Shodex (Showa Denko K.K., Tokyo,Japan). The film density was measured by a hydrostatic weighing method using an AD-1653 specific gravity measuring kit (A&D Company, Tokyo, Japan), with each experiment repeated four times.

Thermogravimetric analysis (TGA) was performed using a TGA 500 instrument (TA Instruments, New Castle, DE, USA) in the range of 30–800 °C, at a heating rate of 10 °C min^{-1}. Differential scanning calorimetry (DSC) was performed using a DSC Q1000 instrument (TA instruments, New Castle, DE, USA) in the range of − 50–250 °C, at a heating rate of 10 °C min^{-1}, under nitrogen atmosphere. Dynamic modulus analysis (DMA) was performed using a Q800 dynamic mechanical analyzer (TA instruments, New Castle, USA) in the range of − 100–200 °C, at a heating rate of 5 °C min^{-1} and a frequency of 1 Hz.

Synchrotron WAXS experiments were performed at a 9 A beamline in Pohang Accelerator Laboratory (PAL), Korea. A monochromatized X-ray radiation source of 11.08 keV (λ = 0.11179 nm) with a sample-to-detector distance (SDD) of 212.23 mm was used. The scattering intensity was collected using a Mar 165 mm diameter CCD detector (2048 × 2048 pixels). The two-dimensional scattering patterns were azimuthally integrated to obtain one-dimensional profiles, presented as the scattering vector (q) versus scattering intensity, where the scattering vector was calculated from the equation $q = 4\pi\lambda/\sin\theta$. The domain spacing ($d$) was calculated from the position of the scattering peaks using the relationship $d = 2\pi/q$. The fractions of amorphous ($F_{amorphous}$) and ordered ($F_{ordered}$) domains were calculated using the equations $F_{amorphous} = A_{amorphous}/A_{total} \times 100\%$ and $F_{ordered} = (A_{crystalline\ 1} + A_{crystalline\ 2} + A_{liquid\ crystalline})/A_{total} \times 100\%$, respectively, where $A_{total} = A_{amorphous} + A_{crystalline\ 1} + A_{crystalline\ 2} + A_{liquid\ crystalline} + A_{\pi\text{-}\pi\ stacking}$.

The dielectric properties of the polyimide films were measured using an E5080B network analyzer (Agilent Technologies, Santa Clara, CA, USA). To verify the dielectric properties of the polymers depending on the frequency, the measurements were performed at frequencies of 10, 28, and 40 GHz. The temperature-dependent dielectric properties of the co-PI-1, 3, and 5 were tested by utilizing metal-insulator-metal (MIM) capacitor assembly and E4980A precision LCR meter (Agilent Technologies, Santa Clara, CA, USA). To fabricate the MIM capacitor, 5 wt% polymer solution in toluene was spin-casted on the SI wafer with targeting 500 nm thickness. Then, 50 nm of the aluminum electrode was deposited on the polymer layer via thermal vapor deposition with 2.0 Å s^{-1}. The dielectric constant and loss value was obtained at a 1 MHz frequency.

2.3. Synthesis of the polyimides

The polyimides were synthesized according to a previously reported two-step thermal imidization process [22]. As a representative example, the copolyimide sample co-PI-3 was prepared as follows: Priamine 1075 (7.4900 g, 0.014 mmol) and mTB (1.2738 g, 0.0060 mmol) were dissolved in cyclohexanone (65.1902 g) in a three-neck round-bottom flask equipped with a condenser and dean stark trap and stirred using an overhead mechanical stirrer under nitrogen atmosphere for 1 h. BPADA (10.4098 g, 0.0200 mmol) was then added to the mixture and stirred at 20 °C to form a pale-yellow poly(amic acid) solution. After 12 h of reaction, toluene (11.5042 g) was added to the solution for azeotropic distillation to promote the thermal imidization process. The mixture was heated to 180 °C and stirred for 4 h to ensure complete imidization. The polyimides were obtained by casting the solution on a Teflon plate and evaporating the solvent by heating the solution to 250 °C under a vacuum for 3 h to produce a brown solid. An identical procedure was used

for the synthesis of the other polyimides with different dimer diamine/mTB ratios (see Table 1).

2.4. Polyimide film fabrication

An identical procedure was used to prepare all the polyimide films in this study. As a representative example, the co-PI-3 film was prepared as follows: A 30 wt% polymer solution of co-PI-3 was prepared by dissolving the polymer in toluene at 20 °C. The solution was cast on a glass plate using a doctor blade film applicator with a thickness of 1000 μm. The cast solution was dried for 6 h under ambient conditions to evaporate the toluene. Subsequently, the film was further dried under vacuum at 80 °C for 12 h to eliminate the residual toluene from the cast solution. The resulting film was obtained by simply detaching it from the substrate.

3. Result And Discussion

3.1. Synthesis of the copolyimides

A series of PIs were prepared via nucleophilic addition between the mTB/Priamine 1075 mixture and BPADA followed by thermal imidization, as shown in Scheme 1 (see the Methods section for synthetic details). The polymers were denoted as co-PI-xx according to the molar fraction of mTB in the reaction mixture. For example, the co-PI containing 30 mol% mTB was labeled co-PI-3. The detailed compositions of these polymers are listed in Table 1. Because BPADA, which comprises flexible ether linkage, was used as the counterpart, all the polyimides were fully soluble in common organic solvents, such as acetone, chloroform, THF, and toluene, suggesting facile solution processability. Based on these results, PI films with uniform thicknesses in the range of 150–200 μm were successfully prepared by uniformly casting a 30 wt% polymer solution in toluene using a doctor blade (Fig. S1). The bulk density of the copolyimide was measured using the hydrostatic weighing method (Table 2). The density proportionally increased with increasing mTB content from 1.07 to 1.13, suggesting a noticeable decrease in the free volume.

The chemical structures of the resulting polymers were determined using ^{1}H NMR and FT-IR spectroscopy (Fig. 1). In the FT-IR spectra, signals at 1710 and 1770 cm^{-1} were assigned to C═O stretching (symmetric and asymmetric imides, respectively), while the signal at 1360 cm^{-1} was assigned to C–N stretching. Signals assigned to methyl and aromatic C–H stretching were also observed at approximately 2850 and 2920 cm^{-1}, respectively. The absence of amine and amide signals near 3300 and 1660 cm^{-1} suggested that no remaining monomers were present in the product, and that the poly(amic acid)s were successfully converted to polyimides.

Table 1
Composition of the reaction mixture for the polyimides synthesized in this study.

Entry	BPADA (g)	Dimer diamine (g)	mTB (g)	mTB (mol %)	Cyclohexanone (mL)	Toluene (mL)
co-PI-0	10.4098	10.7000	0.0000	0	75.7	14.6
co-PI-1	10.4098	9.6300	0.4250	10	73.4	14.2
co-PI-2	10.4098	8.5600	0.8490	20	71.8	13.7
co-PI-3	10.4098	7.4900	1.2740	30	68.8	13.3
co-PI-4	10.4098	6.4200	1.6980	40	66.5	12.8
co-PI-5	10.4098	5.3500	2.1230	50	64.1	12.4

The aliphatic protons of Priamine and aromatic protons of BPADA were assigned from the ^{1}H NMR spectrum of co-PI-0 (Fig. 1b, light-blue). Peaks corresponding to the mTB moiety appeared at 2.08, 7.08, 7.47, and 7.92 ppm, which intensified with increasing mTB molar fraction in the reaction mixture. The final composition of the diamines was estimated from the ratio between the mTB methyl protons at 2.08 ppm and Priamine 1075 methylene protons at 3.56 ppm, as summarized in Table 2. The molar ratio of the diamines well corresponded with the diamine feed ratio, suggesting that polyimides with controlled aliphatic/aromatic segment fractions were synthesized. The molar mass of the polyimide was estimated using size-exclusion chromatography with THF as the eluting solvent (Fig. 1c). The number average molecular weight (M_n) and dispersity ($Đ$) of the resulting polymers were in the range of 9.0–14.9 kg mol^{-1} and 2.69–2.92, respectively. Therefore, we concluded that polyimides with comparable molar masses and distributions were successfully prepared.

3.2. Dielectric properties of the copolyimides

The dielectric constants (D_k) and losses (D_f) of the polyimide free-standing films (5.0 × 5.0 cm^2) were determined at 10, 28, and 40 GHz under ambient conditions (Fig. 2 and Table 3). The PI films were dried under a vacuum prior to measurement (see Experimental section for details). At 10 GHz, the D_k value varied as the composition of the diamines in the polymer backbone was increased from 2.59 to 2.72. Notably, D_k decreased with increasing Priamine 1075 content, regardless of the measuring frequencies. This indicates that the bulky aliphatic side group is effective in increasing the free volume, which is consistent with the observed decrease in the film density (Table 2). In addition, the rich aliphatic composition of the polymer backbone helps reduce the number of polarizable units. The D_k value also decreased when higher measuring frequencies (28 and 40 GHz) were employed, which is known for the changing response of the dipole moments to the external electromagnetic waves [17–19]. Despite of the change in the value, the proportional change of D_k versus the mTB composition remained identical. In contrast to D_k, the D_f values were barely affected by the change in the measuring frequency. A noticeable trend of the D_f against the mTB molar fraction was observed, wherein the D_f decreases until 30 mol% mTB and then increased again with a further increase in mTB. Regardless of the measuring frequencies, the minimum D_f value was always appeared at 30 mol%. These minimum values were 36% and 33% lower than those of co-PI-0 and co-PI-5, respectively. These results suggest that there is an optimal mTB molar fraction that is effective in preventing unexpected energy dissipation via chain relaxation. However, the role of the aromatic units in minimizing the D_f has not yet been fully explored and should be studied for the future design of high-performance polymer materials.

3.3. Thermal properties of the copolyimides

To understand the design factor of the copolymer affecting the dielectric properties, we proceeded to probe the thermal behavior and molecular packing structure of the copolyimides and compared them to those of co-PI-0 as reference. The thermal stabilities of the PIs synthesized in this study were determined by TGA, DSC, and TMA. As shown in Fig. 3a, the polymers exhibited negligible weight loss up to 440 °C, regardless of the diamine composition. Thermal decomposition was observed at temperatures over 443 °C in the case of co-PI-0 and gradually increased from 440° to 496°C with increasing mTB composition in the polymer backbone. The rigidity of the mTB segment was also reflected in the change in the glass transition temperature (T_g) attained from the DSC measurements (Fig. 3b). Indeed, the T_g of the polyimides ranged from 26.6° to 79.7°C without other thermal transitions. These

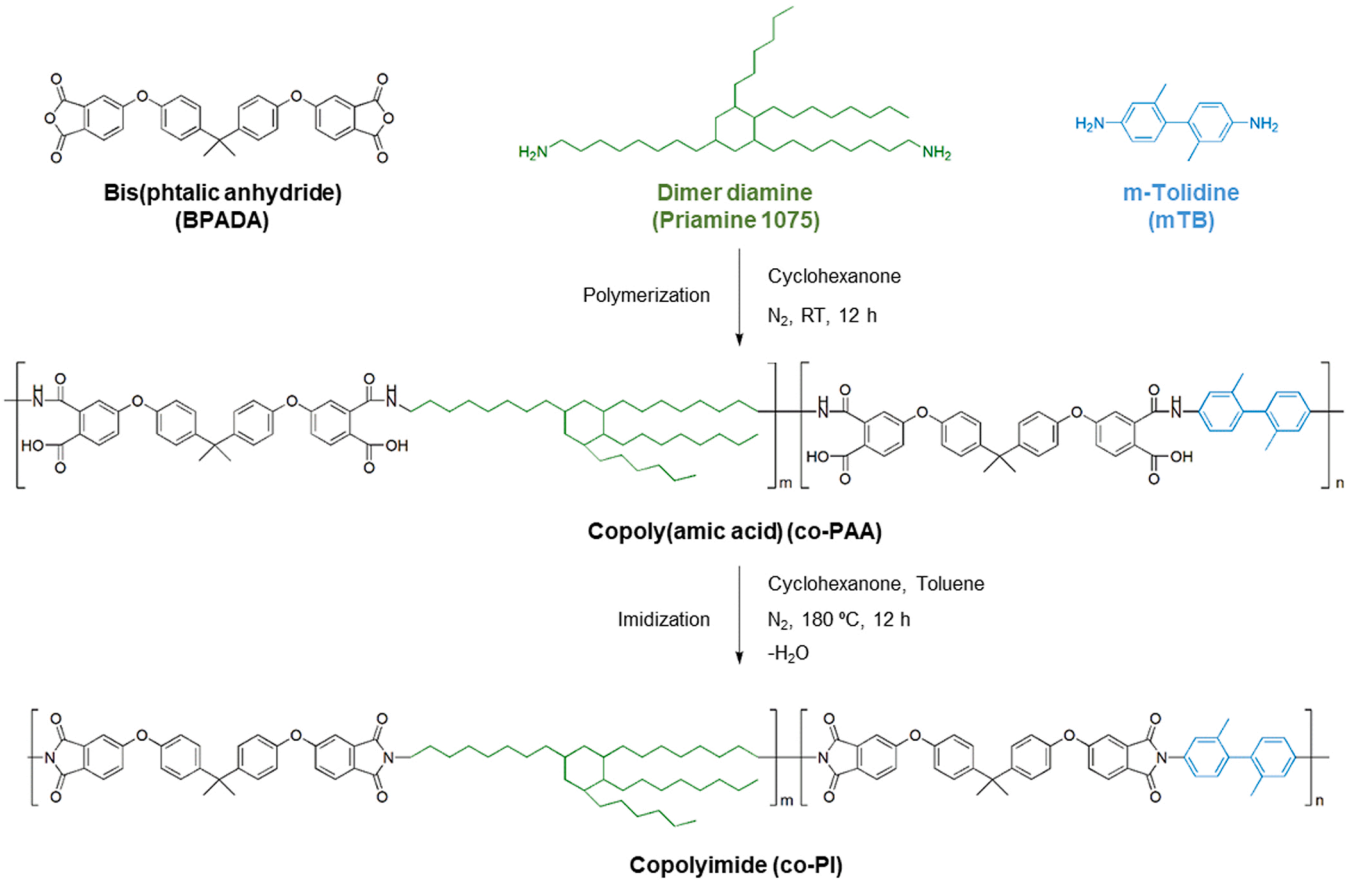

Scheme 1. Synthetic procedure of the copolyimides.

Table 2
Characterization of the chemical structures and thermal properties of the copolyimides.

Name	mTB content (mol%)[a]	M_n (kg mol^{-1})	$Đ$	Density (g cm^{-3})[b]	T_d (°C)[c]	T_g (°C)[d]	T_α (°C)[e]
co-PI-0	0	8.8	2.92	1.07	443	26.6	44.4
co-PI-1	10.1	12.7	2.82	1.08	465	36.2	52.8
co-PI-2	20.2	11.9	2.74	1.10	465	43.1	65.6
co-PI-3	33.0	14.3	2.76	1.11	466	52.9	80.4
co-PI-4	42.5	13.0	2.68	1.13	469	65.9	93.7
co-PI-5	52.8	14.9	2.69	1.13	496	79.7	110.2

[a] Estimated by comparing the peak intensity from the ^{1}H NMR spectrum.
[b] Measured by the hydrostatic weighing method.
[c] Measured by thermal gravimetric analysis.
[d] Measured by differential scanning calorimetry.
[e] Measured by dynamic modulus analysis.

results suggest that the incorporation of the aromatic segment into the polymer backbone effectively prevents thermal deformation, although the T_g values of the resulting polymers are lower than those of the aromatic polyimides (T_g >200 °C).

The polymer chain relaxation was further investigated by DMA in the temperature range of − 100–200 °C with an operating frequency of 1 Hz. At the beginning of the measurement (−100 °C), the storage modulus (E') was enhanced, depending on the mTB composition (Fig. 3c). Thus, the modulus of co-PI-5 was nearly twice that of co-PI-0. As the temperature increased, a sharp drop in E' corresponding to α-chain relaxation was observed, owing to the transition from a glassy to a rubbery state. The α-chain relaxation temperature (T_α) was varied in the range of 40–110 °C as a function of the mTB content. Notably, these results exhibited an identical trend to that of the T_g (26.6–79.7 °C) results attained from DSC analysis, but with a variation in the absolute values of the temperature. In addition, the loss factor (tan δ) corresponding to the α-chain relaxation was shifted to a higher temperature and became wider with increasing mTB composition (Fig. 3d). The enhancement of thermal stability by introducing an aromatic unit is also double confirmed in the D_k and D_f values versus the temperature. The thermal stability of dielectric properties against to the temperature was tested by varying temperatures from 25 to 95 °C with 2.5 °C intervals at 1 MHz of the input frequency (Fig. S2). The D_k retains the nearly constant value under the change of temperature for all the measuring polymers, while the D_f value becomes unstable and increased when the temperature exceeded the T_α. It is noticeable that the co-PI-5 with the highest T_α value showed a wide stable temperature range until 95 °C. These thermal relaxation behaviors of the copolyimides indicated that the rigid aromatic moieties strongly reinforced the resistivity of the polymer against the external environment. This was presumably achieved by the enhancement of the chain rigidity and interchain interactions via non-covalent interactions. Therefore, we supposed that suppression of the chain movement is effective in preventing undesired energy dissipation, resulting in a low D_f at 30 mol% mTB. However, the upturn in D_f for composition exceeding 30 mol% mTB is still not fully explained by the thermal behavior of the copolyimides.

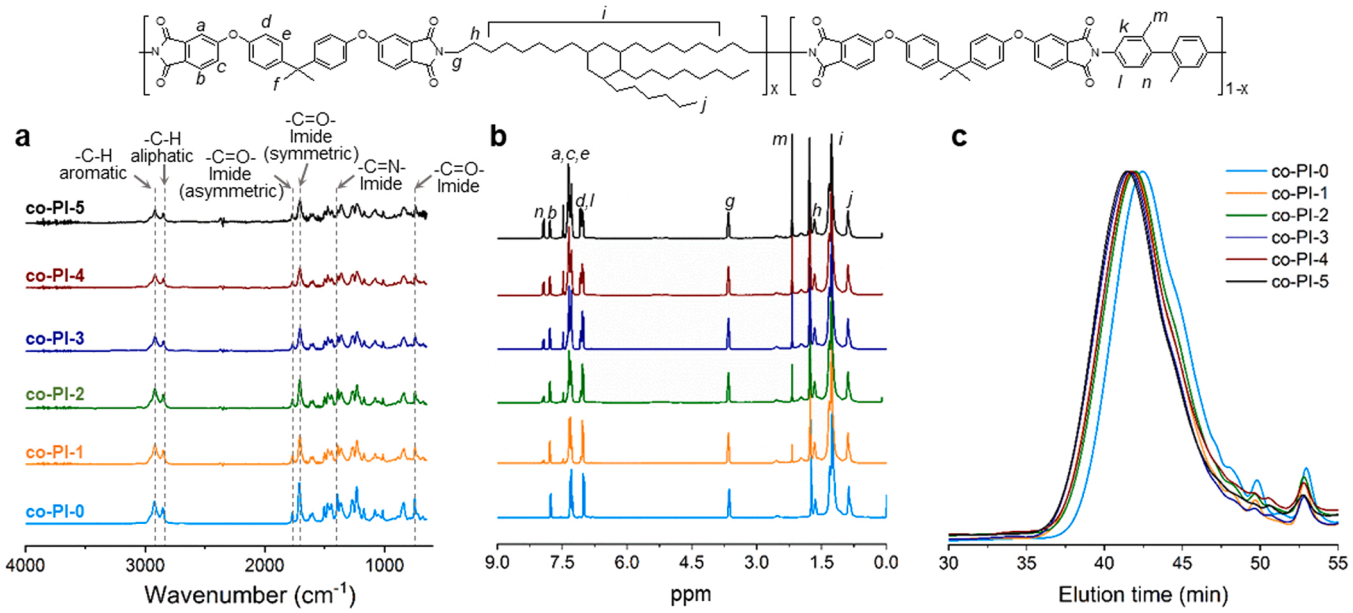

Fig. 1. Characterization of the synthesized copolyimides using (a) FT-IR, (b) ^{1}H NMR, and (c) SEC data.

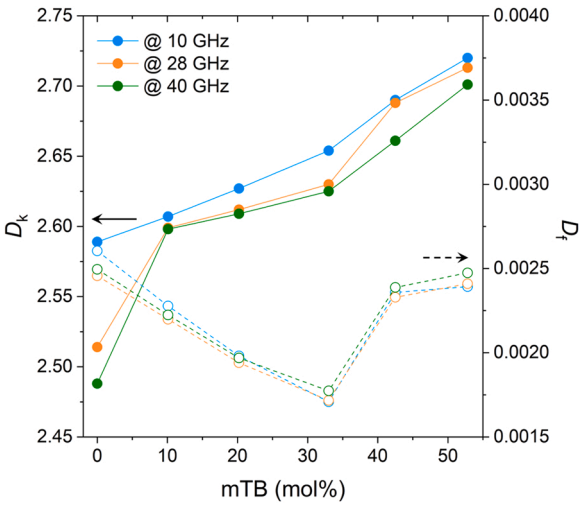

Fig. 2. A plot of the dielectric constant (D_k, solid circles) and dielectric loss factor (D_f, open circles) versus the mTB molar fraction of the copolyimide. The dielectric properties were obtained using a network analyzer at 10 (blue), 28 (orange), and 40 (green) GHz.

3.4. Chain packing structure of the copolyimides

To obtain further insight into the relationship between the nanostructure and dielectric properties, the chain packing structure of the polyimide was studied by synchrotron WAXS (Fig. 4a and S3). Transmission WAXS experiments were performed on the copolyimide bulk films under ambient conditions. Typically, the scattering patterns from the copolyimide were fitted using a previously reported liquid-crystalline model [23]. The average scattering intensity was deconvoluted by assuming a Gaussian peak shape (Fig. S3), and the specific d-spacing ($d = 2\pi/q$) was calculated from the centered peak position (see Table S1).

Representative WAXS data for the copolyimides are shown in Fig. 4a. The co-PI-0 sample presented a broad scattering pattern that mostly originated from the amorphous halo. As the mTB content in the polymer backbone changed, discernible changes in the scattering patterns were observed. For all the copolyimides, the scattering profile at 1.3 Å^{-1} was deconvoluted into the two peaks with distinguishable centered positions and a full width at half maximum (FWHM) (Fig. S4a and Table S1). The broad scattering near 1.30 Å^{-1} ($d = 4.8$ Å) with 0.9–1.2 Å^{-1} FWHM was assigned as an amorphous halo. The narrow scattering at 1.33 Å^{-1} ($d = 4.72$ Å) with 0.3–0.5 Å^{-1} FWHM is the liquid crystalline domain, which falls within the range of the typical interchain packing of aromatic polyimides. The weaker scattering at $q = 0.35$ Å^{-1} ($d = 18.0$ Å) is presumably the ordered packing originating from the length of the alternating dianhydride and diamine moieties. These scattering profiles indicate that the ordered nanodomains are dispersed in the amorphous polymer matrix, suggesting that the as-synthesized copolyimide comprises semicrystalline nanostructures.

The fraction of ordered and amorphous domains was determined by calculating the ratio between the area of each scattering intensity and the total scattering profile (Fig. 4b and S3; see the Methods section for calculation details). Notably, the ordered fraction contains every crystalline and liquid crystalline area, except for π–π stacking. When the

Table 3
Characterization of the chemical structures and thermal properties of the copolyimides.

Name	D_k			D_f		
	@ 10 GHz	@ 28 GHz	@ 40 GHz	@ 10 GHz	@ 28 GHz	@ 40 GHz
co-PI-0	2.59	2.51	2.49	0.0026	0.0025	0.0025
co-PI-1	2.61	2.60	2.60	0.0023	0.0022	0.0022
co-PI-2	2.63	2.61	2.61	0.0020	0.0019	0.0020
co-PI-3	2.65	2.63	2.63	0.0017	0.0017	0.0018
co-PI-4	2.69	2.69	2.66	0.0024	0.0023	0.0024
co-PI-5	2.72	2.71	2.70	0.0024	0.0024	0.0025

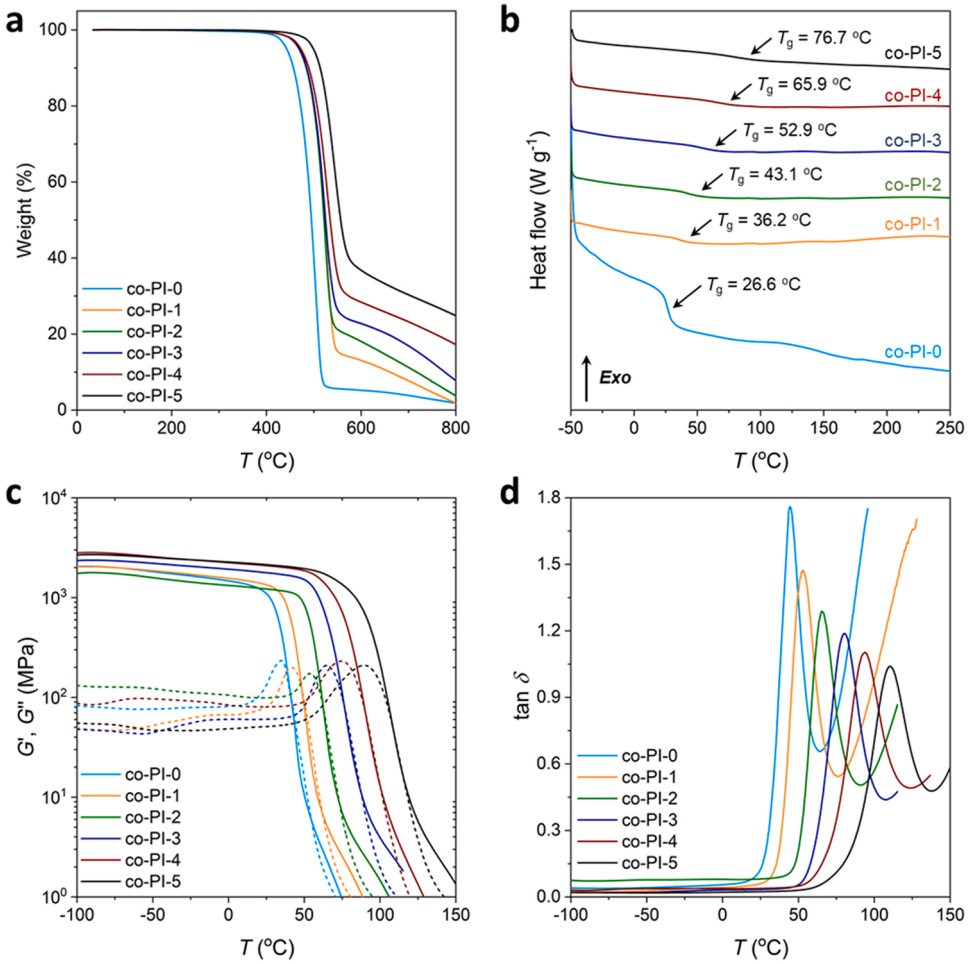

Fig. 3. Thermal analyses of the copolyimides: (a) TGA and (b) DSC traces. Plots of the (c) storage (solid line) and loss (dashed lines) moduli and (d) loss factors (tanδ) obtained by DMA.

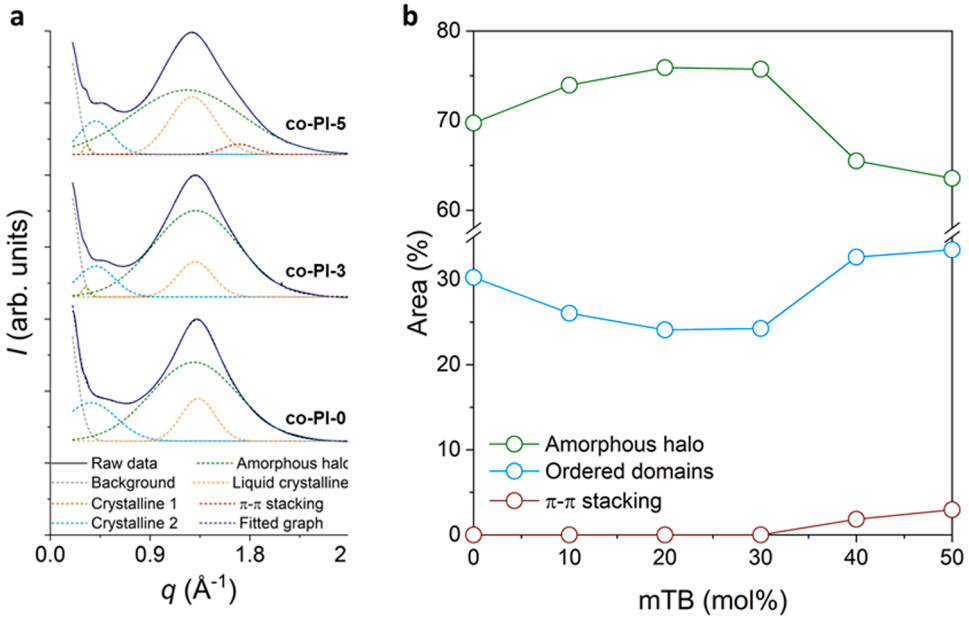

Fig. 4. (a) Representative raw (solid line) and deconvoluted (dashed lines) WAXS data of the copolyimides. (b) Plot of the intensity area fractions of the copolyimides against the mTB molar fractions. The ordered domain includes the liquid crystalline and crystalline components of the deconvoluted scattering profile.

mTB content reached 30 mol%, the copolyimide showed the highest amorphous fraction (75.7%) in the series. This is related to the randomness of the polymer backbone, which was also confirmed by the increase in the FWHM (Fig. S3b). However, when the mTB population exceeded 40 mol%, the scattering intensity from the amorphous halo was reduced, while the fraction of ordered domains increased. In addition, the peaks near 0.3, 0.4, and 1.7 $Å^{-1}$ corresponding to the crystalline and π–π stacking distances become evident. This suggests that the interchain interactions between the polymer chains are enhanced via aromatic–aromatic interactions, including π–π stacking, as the aromatic moiety in the polymer backbone is enriched. As a result, the polymer matrix comprises a more ordered nanostructure with a dense matrix that resists thermal and mechanical deformation [19].

Based on these observations, we estimated the correlation between the chemical structure of the polymer backbone and the dielectric properties: Priamine 1075 has a significant advantage in reducing the D_k value of the polymer material. The aliphatic chains reduce the intrinsic dipole moments of the polymer backbone, resulting in a reduction in D_k. In addition, the branched side chains enlarge the free volume between the polymer backbone by steric hindrance, thereby reducing the bulk density and maintaining the polymer materials soft and amorphous (co-PI-0; Fig. S3 and Table 2). However, the steric effect of the aliphatic side chains also decreases the T_α to 40 °C, as shown in Fig. 3a. This severely affects the D_f value because the chain relaxation process is known as the critical factor of electromagnetic energy loss [18,19]. As a result, the polyimide solely comprising Priamine 1075 (co-PI-0) displayed a low D_k of 2.51 and high D_f of 0.0025 value at 28 GHz (Fig. 2 and Table 3).

The introduction of an aromatic mTB unit changed both the dielectric properties and chain-packing structure. Compared to the branched aliphatic units, mTB has a planar chemical structure that promotes interchain packing by densifying the polymer material (Table 2). The intrinsic dipole moment of the aromatic unit also increases the population of the effective dipole moment. These changes led to an increase in D_k, proportional to the mTB composition (Fig. 2, solid line). On the other hand, D_f was at a minimum at 30 mol% mTB (Fig. 2, dashed line). These results suggest that the introduction of aromatic units suppresses energy dissipation even though the dipole population increases. At the same time, increasing the T_g of polyimide is a valid strategy to reduce the D_f by preventing the energy dissipation through the chain motions. As described above, the introduction of mTB effectively increased the T_g from 26.6° to 76.7°C, indicating that the chain movement is arrested by the addition of aromatic units. In addition, the nanostructure of the copolyimide was more amorphous in co-PI-3 because of the randomness of the polymer repeating units (Fig. 4b and S2). These results indicate that the copolyimide with 10–30 mol% of mTB is a rigid amorphous polymer with restricted chain motion. Therefore, the D_f was effectively decreased and reached to 0.0017 in co-PI-3, which is 36% lower than that of co-PI-0. This suggests that the prevention of chain relaxation is essential for lowering electromagnetic energy loss. Moreover, the increase in D_f after 40 mol% aromatic units is presumably caused by the formation of densely packed aromatic domains (Fig. 4b). We believe the complex factors including aromatic ring density, imide group density, bulk density, and interchain interactions affect to increase of the D_f value after mTB 40 mol% [2,5]. Our aliphatic-aromatic results suggest that there is an optimal ratio showing an adequate level of D_k with the lowest D_f value. This optimal ratio is closely related to the effective dipole density, chain rigidity, and polymer nanostructure. Therefore, the design of the copolyimides should consider both the optimal composition and the combination of the monomers.

4. Conclusion

We synthesized low-dielectric copolyimides by copolymerizing an aromatic dianhydride with branched aliphatic and aromatic diamines. Our polymer design achieved D_k values of 2.5–2.7 and D_f values of 0.0017–0.0025 at 28 GHz, which were tuned according to the diamine ratio in the polymer backbone. The branched aliphatic chain helped enlarge the inter-chain space to reduce the effective number of dipole moments, while the chain relaxation temperature decreased to approach the RT. Although the number of dipole moments increases proportionally with the increases in aromatic moiety, their non-covalent interactions effectively inhibit chain motion, resulting in a reduction in the dielectric loss. The molar fraction between the diamines that minimized the D_f value was strongly correlated with the chain relaxation behavior and chain packing structure, as observed from the DMA and WAXS data. For the copolymer comprising Priamine 1075 and mTB, 30 mol% mTB was the optimal ratio with a D_k of 2.63 and D_f of 0.0017 at 28 GHz. Our results suggest that there is an optimal copolyimide molar fraction to achieve the lowest D_f value while minimizing the increase in the D_k value of the polymer film. Therefore, the design of a copolymer with a reduced effective dipole moment and chain motion should be considered to achieve polymer materials for next-generation telecommunication applications.

Funding Sources

This study was supported by KRICT core project (no. SS2221–20), the National Research Foundation of Korea (NRF) grant funded by the Ministry of Science and ICT, Korea (MSIT, NRF-2021M3H4A3A01045740), and Korea Evaluation Institute of Industrial Technology (KEIT) grant funded by the Ministry of Trade, Industry and Energy, Korea (MOTIE, KEIT-20014103). Experiments at 9 A beamline of Pohang Accelerator Laboratory (PAL) were supported in part by MSIT and POSTECH.

CRediT authorship contribution statement

Jiwon Lee: Investigation, Methodology, Writing – original draft, Formal analysis, Visualization. **Sungmi Yoo:** Methodology, Investigation, Formal analysis, Writing – review & editing. **Yun Ho Kim:** Methodology, Resources, Writing – review & editing. **Sungmin Park:** Methodology, Writing – review & editing. **No Kyun Park:** Writing – review & editing. **Yujin So:** Validation, Writing – review & editing. **Jinsoo Kim:** Validation, Resources, Writing – review & editing. **Jongmin Park:** Methodology, Formal analysis, Investigation, Writing – original draft, Visualization, Supervision. **Min Jae Ko:** Validation, Writing – review & editing, Project administration. **Jong Chan Won:** Conceptualization, Validation, Resources, Writing – original draft, Supervision, Project administration.

Declaration of Competing Interest

The authors declare that they have no known competing financial interests or personal relationships that could have appeared to influence the work reported in this paper.

Data Availability

No data was used for the research described in the article.

Appendix A. Supporting information

Supplementary data associated with this article can be found in the online version at doi:10.1016/j.mtcomm.2022.104479.

References

[1] Z., M. Temesvári, D. Maros, P. Kádár, Review of mobile communication and the 5G in manufacturing, Procedia Manuf. 32 (2019) 600–612.
[2] L. Tang, J. Zhang, Y. Tang, J. Kong, T. Liu, J. Gu, Polymer matrix wave-transparent composites: a review, J. Mater. Sci. Technol. 75 (2021) 225–251.
[3] G. Maier, Low dielectric constant polymers for microelectronics, Prog. Polym. Sci. 26 (2001) 3–65.

[4] D. Shamiryan, T. Abell, F. Iacopi, K. Maex, Low-k dielectric materials, Mater. Today 7 (2004) 34–39.
[5] C.-C. Kuo, Y.-C. Lin, Y.-C. Chen, P.-H. Wu, S. Ando, M. Ueda, W.-C. Chen, Correlating the molecular structure of polyimides with the dielectric constant and dissipation factor at a high frequency of 10 GHz, ACS Appl. Polym. Mater. 3 (2020) 362–371.
[6] S.M.R. Billah, Dielectric Polymers, in: M.A. Jafar Mazumder, H. Sheardown (Eds.), A. Al-Ahmed Functional Polymers, Springer International Publishing, New York, 2018, pp. 241–288.
[7] M.K. Ghosh, K.L. Mittal, Polyimide: fundamentals and applications, Marcel Dekker Inc, New York, 1996.
[8] D.-J. Liaw, K.-L. Wang, Y.-C. Huang, K.-R. Lee, J.-Y. Lai, C.-S. Ha, Advanced polyimide materials: synthesis, physical properties and applications, Prog. Polym. Sci. 37 (2012) 907–974.
[9] W. Volksen, R.D. Miller, G. Dubois, Low dielectric constant materials, Chem. Rev. 110 (2010) 56–110.
[10] S. Park, H.Y. Chang, S. Rahimi, A.L. Lee, L. Tao, D. Akinwande, Transparent nanoscale polyimide gate dielectric for highly flexible electronics, Adv. Electron. Mater. 4 (2018) 1700043.
[11] S. Han, Y. Li, F. Hao, H. Zhou, S. Qi, G. Tian, D. Wu, Ultra-low dielectric constant polyimides: Combined efforts of fluorination and micro-branched crosslink structure, Eur. Polym. J. 143 (2021), 110206.
[12] A.M. Joseph, B. Nagendra, K. Surendran, E. Bhoje Gowd, Syndiotactic polystyrene/hybrid silica spheres of POSS siloxane composites exhibiting ultralow dielectric constant, ACS Appl. Mater. Interfaces 7 (2015) 19474–19483.
[13] Y. Zhuang, J.G. Seong, Y.M. Lee, Polyimides containing aliphatic/alicyclic segments in the main chains, Prog. Polym. Sci. 92 (2019) 35–88.
[14] Y.-T. Chern, Low dielectric constant polyimides derived from novel 1,6-bis [4-(4-aminophenoxy) phenyl]diamantane, Macromolecules 31 (1998) 5837–5844.
[15] Y. Liu, C. Qian, L. Qu, Y. Wu, Y. Zhang, X. Wu, B. Zou, W. Chen, Z. Chen, Z. Chi, A bulk dielectric polymer film with intrinsic ultralow dielectric constant and outstanding comprehensive properties, Chem. Mater. 27 (2015) 6543–6549.
[16] Y. Watanabe, Y. Shibasaki, S. Ando, M. Ueda, Synthesis of semiaromatic polyimides from aromatic diamines containing adamantyl units and alicyclic dianhydrides, J. Polym. Sci. Part A: Polym. Chem. 42 (2004) 144–150.
[17] P. Avakian, H.W. Starkweather Jr., W.G. Kampert, Dielectric analysis of polymers, in: S.Z.D. Cheng (Ed.), Handbook of thermal analysis and calorimetry Vol 3: Applications to polymers and plastics, Elsevier, Amsterdam, 2002, pp. 147–165.
[18] Z. Ahmad, Polymer dielectric materials, in: M.A. Silaghi (Ed.), Dielectric Material, IntechOpen, London, 2012, https://doi.org/10.5772/50638.
[19] D.F. Miranda, S. Zhang, J. Runt, J. Controlling crystal microstructure to minimize loss in polymer dielectrics, Macromolecules 50 (2017) 8083–8096.
[20] A. Susa, J. Bijleveld, M.H. Santana, S.J. Garcia, Understanding the effect of the dianhydride structure on the properties of semiaromatic polyimides containing a biobased fatty diamine, ACS Sustain. Chem. Eng. 6 (2018) 668–678.
[21] S. Miyane, C.-K. Chen, Y.-C. Lin, M. Ueda, W.-C. Chen, Thermally stable colorless copolyimides with a low dielectric constant and dissipation factor and their organic field-effect transistor applications, ACS Appl. Polym. Mater. 3 (2021) 3153–3163.
[22] A. Susa, R. Bose, A.M. Grande, S. van der Zwaag, S.J. Garcia, Effect of the dianhydride/branched diamine ratio on the architecture and room temperature healing behavior of polyetherimides, ACS Appl. Mater. Interfaces 8 (2016) 34068–34079.
[23] J. Wakita, S. Jin, T.J. Shin, M. Ree, S. Ando, Analysis of molecular aggregation structures of fully aromatic and semialiphatic polyimide films with synchrotron grazing incidence wide-angle X-ray scattering, Macromolecules 43 (2010) 1930–1941.